Contribution from the Department of Chemistry,
University of Michigan, Ann Arbor, Michigan 48103

Platinum and Palladium Complexes of Thienylpyridine. I. Compounds Containing Metal–Carbon Bonds

T. J. GIORDANO and PAUL G. RASMUSSEN*

Received October 22, 1974 AIC40725Q

Complexes of divalent platinum and palladium with 2-(2'-thienyl)pyridine (TP) have been investigated. In this paper we describe the syntheses and structures of those derivatives which form a metal–carbon σ bond by the spontaneous loss of a hydrogen from an aromatic group (TP-H). The reaction of TP with PtX_4^{2-} ($X = Br^-, I^-$) yields orange crystalline Pt(TP)(TP-H)X. In these complexes, one TP acts as a monodentate N donor and the other as an N–C chelate, through the thienyl ring. A yellow, crystalline palladium analog Pd(TP)(TP-H)NO_3 can be prepared by the reaction of TP with $AgNO_3$ and PdI_4^{2-}. All of these complexes are monomers and nonelectrolytes in nonpolar solvents. The crystal structure of iodo[2-(2'-thienyl)pyridine][2-(2'-thienyl)pyridyl]platinum(II) was determined from three-dimensional single-crystal X-ray diffraction data collected by counter methods. The complex $Pt(C_9H_7NS)(C_9H_6NS)I$ was found to crystallize in the monoclinic space group $P2_1/n$ with $a = 17.360$ (3) Å, $b = 8.418$ (1) Å, $c = 13.556$ (2) Å, $\beta = 110.53$ (2)°, $Z = 4$ molecules/cell. The structure was refined by block diagonal and full matrix methods to a final R factor of 4.6% for 2220 nonzero reflections. The platinum atom is coordinated by two pyridyl nitrogens trans to one another, a thienyl carbon, and an iodide which lies slightly below the plane formed by the platinum and the other three coordinating atoms. The Pt–N distances are 2.04 (1) and 2.02 (1) Å for the nitrogens in the monodentate and the chelated ligands, respectively; the Pt–I and Pt–C distances are 2.68 (1) and 1.97 (2) Å, respectively. The free thiophene ring (not coordinated to the metal by a metal–carbon σ bond) is in an axial position. This ring was found to be disordered by 180° rotation about the pyridine–thiophene bond. The Pt–S distance (2.99 (3) Å) was nevertheless determined with reasonable accuracy and was found to be less than the sum of the van der Waals radii. The line between the platinum and the sulfur makes an angle of ca. 15° with the normal to the equatorial plane at the platinum site. The visible–ultraviolet spectra of these complexes resemble the spectra of five-coordinate d^8 complexes and the ir spectra show a shifted thiophene band assigned to the thiophene ring in the axial position. These spectral results are interpreted with respect to metal–thiophene axial interaction. The metal to carbon σ bond forms with unusual ease under wet, aerobic conditions due to the thiophene ring reactivity and the chelate stability.

Introduction

Although several purported metal–thiophene sulfur linkages exist in the literature, none are well documented. On the other hand the α carbons are readily substituted by certain metals and compounds such as

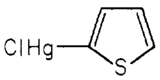

have long been known. The molecule 2-(2'-thienyl)pyridine

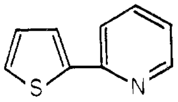

2-(2'-thienyl)pyridine

offers the possibility of testing a weak binding tendency, by taking advantage of chelate stability, even though direct monodentate tests of thiophene complexation have failed. Reactions in which phenyl rings bonded to n-donor or p-donor ligands undergo electrophilic aromatic substitution by platinum(II) and palladium(II), have been the subject of recent research.[1] Azobenzene, for example, reacts with methanolic $PdCl_2$ and K_2PtCl_4 to form dimeric chlorine-bridged complexes.[2]

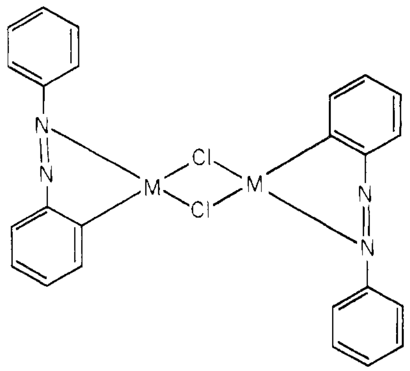

These dimers react with amines and phosphines to form monomeric complexes of formula M(azo-H)LCl. Dimers, analogous to the azobenzene compounds, have also been prepared using such ligands as 2-phenylpyridine[3] and *N*,*N*-dimethylbenzylamine.[4]

Cheney[5] et al. have reported that substitution of a phenyl ring by the platinum occurs when complexes of formula *trans*-$Pt(PR_2C_6H_5)_2X_2$ and *trans*-$Pt(PR(C_6H_5)_2)_2X_2$ are refluxed in dimethoxyethanol. The resulting complexes are monomers of formula $Pt(PR_2(C_6H_4))(PR_2C_6H_5)X_2$ and $Pt(PRC_6H_5(C_6H_4))(PR(C_6H_5)_2)X_2$ respectively.

We have undertaken[6] the synthesis of palladium(II) and platinum(II) complexes of 2-(2'-thienyl)pyridine (TP) to determine the mode of coordination and also to ascertain the effect of an adjacent thienyl group on the coordination of an n-donor ligand.

Experimental Section

Infrared spectra between 4000 and 450 cm^{-1} were recorded on a Perkin-Elmer Model 457 recording spectrometer. The samples were in the form of Nujol mulls placed between KBr or NaCl plates.

Absorption spectra between 7000 and 2300 Å were obtained with a Cary Model 14 spectrophotometer. Methylene chloride solutions of the samples in a 1.0-cm quartz cell were placed in the sample beam; pure solvent in a matching cell was used as a reference.

Nitromethane solutions of the samples were prepared and their conductivities measured on an apparatus described elsewhere.[7]

X-Ray powder photographs were obtained using Ni-filtered Cu Kα radiation. Glass capillary tubes (0.3-mm) containing the samples were mounted in a 114.59-mm Debye–Scherrer camera. The 2θ values were measured directly using a film reader and the d values were obtained by the use of appropriate conversion tables.[8]

Microanalyses were determined by the Spang Microanalytical Laboratory, Ann Arbor, Mich., and by Galbraith Laboratories, Inc., Knoxville, Tenn. Molecular weights were determined in chloroform by Galbraith Laboratories.

Preparation of 2-(2'-Thienyl)pyridine. 2-(2'-Thienyl)pyridine was prepared by the method of Kauffmann[9] with slight modifications.

n-Butyllithium (16% in hexane), 250 ml (0.42 mol), was filtered under nitrogen into a 500-ml three-neck flask. Hexane was removed with a vacuum pump until the volume of liquid remaining was ca.

70 ml. Anhydrous ethyl ether, 250 ml, was added and the mixture transferred to a nitrogen-swept 1-l. three-neck flask equipped with an electric stirrer, a reflux condenser, and a 250-ml pressure-equalized dropping funnel. Thiophene, 25 ml (0.31 mol), dissolved in 100 ml of anhydrous ether, was added dropwise to the *n*-butyllithium solution at a rate sufficient to maintain reflux. The resulting mixture was refluxed for 30 min after the thiophene addition was completed, to complete the formation of thienyllithium.

2-Fluoropyridine, 25 g (0.30 mol), dissolved in 150 ml of anhydrous ether, was added dropwise to the refluxing 2-thienyllithium. The resulting mixture was heated for 2 hr. The reaction mixture was cooled in an ice bath, and the excess *n*-butyllithium destroyed with water. The layers were separated, the water layer was extracted with ether, and the combined ether solutions were dried over anhydrous sodium sulfate.

Ether was removed from the dried solution and the residue was vacuum distilled. During distillation, crude TP sublimed into the condenser from which it was removed. The product was vacuum sublimed at 40–45°. The sublimate was washed with 10 ml of 30–60° petroleum ether (to remove an oil which had condensed along with the product) and air-dried. The melting point is 62–64° (lit.[9] mp 64° dec).

Anal. Calcd for C_9H_7NS: C, 67.08; H, 4.35; N, 8.69; S, 19.88. Found: C, 67.10; H, 4.54; N, 8.60; S, 19.82.

The infrared spectrum showed absorption maxima in the region 900–600 cm^{-1} at 850 (s), 835 (w), 770 (s), 735 (m), and 695 (s) cm^{-1}.

Preparation of Iodo[2-(2'-thienyl)pyridine][2-(2'-thienyl)pyridyl)platinum(II). Potassium tetrachloroplatinate, 0.175 g (0.5 mmol), was dissolved in 10 ml of water. Potassium iodide, 0.35 g (2.1 mmol), dissolved in 10 ml of water was added to it and the mixture was stirred for 6 hr. The solution was filtered and 0.18 g (1.1 mmol) of TP, dissolved in 20 ml of acetone, was added, followed by 40 ml of a 1:1 v/v water–acetone mixture. After brief stirring, the solution was transferred to a glass-stoppered erlenmeyer flask. After several hours, the solution began to turn cloudy. Sufficient acetone was added to just turn the solution clear again. This was repeated over the next 24 hr whenever necessary. By the end of 24 hr, the solution turned from green-brown to deep red. During the course of the next 2 weeks, the color of the solution lightened to orange. By the end of 3 weeks, small crystals had appeared at the bottom of the flask. The glass stopper was replaced by a notched cork to allow slow solvent evaporation. Crystallization was allowed to continue for 4 days before the orange crystals were collected by filtration, washed two times each with 15-ml portions of ethyl ether and 30–60° petroleum ether, and air-dried; yield 30%.

Anal. Calcd for $Pt(C_9H_7NS)(C_9H_6NS)I$: C, 33.58; H, 2.02; mol wt 643. Found: C, 34.18; H, 2.15; mol wt 629.

The infrared spectrum showed absorption maxima in the region 900–600 cm^{-1} at 875 (s), 850 (m), 830 (m), 780 (s), 765 (s), 745 (m), 720 (s), and 695 (s) cm^{-1}.

Preparation of Bromo[2-(2'-thienyl)pyridine][2-(2'-thienyl)-pyridyl]platinum(II). Platinum(II) chloride, 0.266 g (1 mmol), was suspended in 60 ml of acetone. Potassium bromide, 0.5 g (4.2 mmol), dissolved in 10 ml of acetone, was added and the mixture stirred for 5 days. The solution of K_2PtBr_4 was then filtered and 0.36 g (1.3 mmol) of TP was added followed by 80 ml of water. After brief stirring, the mixture was transferred to a glass-stoppered erlenmeyer flask. Within 1 hr, a brown precipitate appeared. By the end of 72 hr, orange crystals had appeared along with the brown powder. The mixture was allowed to stand for 24 more hr, after which the mixture was poured into ca. 400 ml of carbon tetrachloride. Small portions of ethyl ether were added until the orange crystals sank to the bottom of the beaker. The liquid and the brown precipitate, which did not sink, were poured off. The crystals were washed two times each with 50-ml portions of carbon tetrachloride and ethyl ether before the crystals were transferred to a 15-ml sintered-glass funnel. The crystals were washed with 15-ml portions of 30–60° petroleum ether and air-dried. Finally, the crystals were dried in vacuo at 80° for 2 hr; yield 20%.

Anal. Calcd for $Pt(C_9H_7NS)(C_9H_6NS)Br$: C, 36.24; H, 2.18; mol wt 596. Found: C, 35.88; H, 2.30; mol wt 604.

The infrared spectrum showed absorption maxima in the region 900–600 cm^{-1} at 875 (s), 850 (m), 830 (m), 780 (s), 765 (s), 745 (m), 725 (s), and 695 (s) cm^{-1}.

Preparation of Nitrato[2-(2'-thienyl)pyridine][2-(2'-thienyl)-pyridyl]palladium(II). Palladium(II) chloride, 0.177 g (1.0 mmol), was suspended in 50 ml of acetone. Potassium iodide, 0.71 g (4.3 mmol), was added and the mixture was stirred for 5 hr. The mixture was then filtered and 0.36 g (2.3 mmol) of TP was added followed by 1.1 g (6.5 mmol) of silver nitrate dissolved in 10 ml of water. Upon addition of the silver nitrate, the violet solution turned pale yellow and a precipitate of silver halides appeared immediately. The mixture was stirred for 5 hr and filtered. The acetone was allowed to evaporate from the filtrate. The pale yellow material which precipitated was collected by filtration, washed in the manner of the preceding compound, and air-dried. The product was recrystallized by being dissolved in the minimum amount of methylene chloride and the solvent allowed to evaporate until yellow crystals appeared. These were collected by filtration, washed two times each with ethyl ether and 30–60° petroleum ether and air-dried; yield 60%.

Anal. Calcd for $Pd(C_9H_7NS)(C_9H_6NS)(NO_3)$: C, 44.00; H, 2.65; N, 8.57; S, 13.00; mol wt 489. Found: C, 43.98; H, 2.67; N, 8.59; S, 13.10; mol wt 492.

The infrared spectrum showed absorption maxima in the region 900–600 cm^{-1} at 875 (s), 840 (m), 810 (m), 770 (s), 760 (s), 715 (s), and 710 (s) cm^{-1}.

Properties and Spectra. The platinum complexes are soluble in polar organic solvents and in benzene; the palladium complex is less soluble in polar organic solvents than the platinum complex and is insoluble in benzene. All three complexes are nonelectrolytes in nitromethane, and their molecular weights indicate that they are monomers in chloroform solution.

It is shown by X-ray powder patterns that the Pt(TP)(TP-H)I and Pt(TP)(TP-H)Br are isomorphous; $Pd(TP)(TP\text{-}H)NO_3$ is not isomorphous with the platinum complexes.

Crystal Structure Determination of Pt(TP)(TP-H)I

Cell Parameters and Data Collection. The orange crystals of $Pt(C_9H_7NS)(C_9H_6NS)I$ described above were found to be suitable for X-ray examination. An irregular many-sided polyhedral crystal, whose thickness varied from 0.13 to 0.17 mm, was used for precession photographs and the gathering of intensity data.

Precession photographs showed that the crystal was monoclinic. Systematic extinctions were found for $k = 2n + 1$ on $0k0$ and $h + l = 2n + 1$ on $h0l$. These extinctions are consistent with the centrosymmetric space group $P2_1/n$. $P2_1/n$ was chosen instead of $P2_1/c$ because the angle β is closer to 90°. The lattice parameters obtained by the method described below are $a = 17.360$ (3) Å, $b = 8.418$ (1) Å, $c = 13.556$ (2) Å, and $\beta = 110.53$ (2)°. The density of 2.25 g/cm^3, measured by the flotation method in a carbon tetrachloride–bromoform mixture, is in good agreement with the value calculated for 4 molecules/unit cell (2.31 g/cm^3).

The crystal was mounted on a Syntex $P\bar{1}$ automated four-circle diffractometer equipped with a graphite single-crystal monochromator. The c^* axis of the crystal was mounted along the ϕ axis of the instrument. Fifteen diffraction maxima were centered on 2θ, χ, and ϕ. Least-squares refinement was used to obtain the orientation matrix and refined lattice parameters. Standard deviations of the lattice parameters were later obtained by least-squares refinement of the 2θ values of 14 reflections and the lattice parameters.

Intensity data were collected with Mo Kα radiation (λ 0.7107 Å) using a θ–2θ scan with background being counted on both sides of each peak. The scan rate varied from 2°/min when $I < 75$ sec^{-1} to 50°/sec when $I > 750$ sec^{-1} and proportionally between these limits. A standard reflection, measured after each 30 reflections, showed no significant changes in intensity during the data collection. The data set consisted of 6376 reflections collected over the range $0.03 < (\sin \theta)/\lambda < 1.09$. All reflections with intensity less than 3σ intensity were classified as "less thans".

The data were corrected for Lorentz and polarization effects and an absorption correction was made ($\mu = 92.9$ cm^{-1}) based on the approximation of the crystal as a sphere of radius 0.075 mm. Data for the correction were obtained from ref 10. The absorption corrections of the observed structure factors ranged from 2.49 to 2.75, and the estimated error due to absorption was found to be about 4% based on differences in F_o for equivalent reflections.

It was noted that few observed reflections were found at $(\sin \theta)/\lambda$ greater than 0.64. Therefore, only reflections found at $(\sin \theta)/\lambda$ less than this value were used in the refinement. The final data set consisted of 2220 independent observed reflections.

Structure Determination and Refinement. The programs of XRAY 72[11] were used in all calculations except least-squares refinement for

Table I. Final Positional Parameters for Pt(TP)(TP-H)I[a]

Atom	*x/a*	*y/b*	*z/c*
Pt	2164 (0)	2115 (1)	106 (0)
I	1582 (1)	1075 (1)	1576 (1)
N(1)	2934 (8)	261 (16)	157 (10)
C(1)	1983 (11)	3910 (24)	4296 (16)
C(2)	1488 (14)	2672 (30)	4358 (18)
C(3)	1055 (12)	2898 (27)	5061 (16)
C(4)	1096 (12)	4159 (25)	5596 (16)
C(5)	3379 (11)	0382 (24)	9484 (14)
C(6)	3236 (10)	1919 (22)	8938 (14)
C(7)	2666 (10)	2900 (24)	9104 (14)
C(8)	2608 (12)	4334 (24)	8536 (15)
C(9)	3100 (14)	4431 (28)	7958 (18)
S(1)	3705 (4)	2686 (8)	8119 (5)
N(2)	1433 (8)	4044 (16)	9932 (10)
C(10)	3261 (12)	121 (24)	4254 (15)
C(11)	3658 (12)	1595 (26)	4262 (16)
C(12)	4346 (12)	1944 (26)	5155 (16)
C(13)	4659 (12)	873 (25)	5948 (16)
C(14)	737 (9)	4412 (20)	9109 (12)
C(15)	407 (9)	3250 (19)	8271 (12)
C(16)/S(2′)	4757 (9)	1297 (18)	2164 (12)
C(17)/C(18′)	4540 (15)	2925 (34)	1677 (20)
C(18)/C(17′)	−110 (14)	782 (28)	7242 (18)
S(2)/C(16′)	563 (4)	1240 (9)	8449 (6)

[a] All values are $\times 10^4$. Standard errors for last significant figures are given in parentheses here and in subsequent tables.

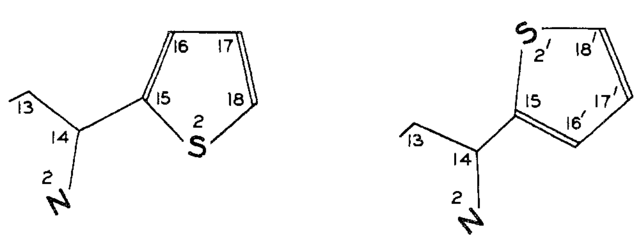

Figure 1. Orientations of the disordered thiophene ring in Pt(TP)(TP-H)I.

which the CLS[12] program was employed. ORTEP[13] was used in drawings of the structure. Scattering factors for Pt(II) and I^- were taken from Cromer and Waber;[14] those for H atoms were from Stewart, Davidson, and Simpson;[15] those for the remaining atoms were from ref 16.

Normalized structure factors were calculated, and a statistical analysis of the data confirmed that the structure was centrosymmetric.

A sharpened, origin-removed Patterson map was calculated from which the platinum atom was located. The iodine atom was located from observations of the Fourier map determined from structure factors calculated for the platinum atom. After the heavy-atom positions were refined (R = 19.3%), a difference Fourier map was calculated from which all of the nonhydrogen atoms were successfully located resulting in an R factor of 13% [$R = \sum(|F_o| - |F_c|/|F_o|)$].

During the first cycles of least-squares refinement, the function minimized was $w\sum(|F_o| - |F_c|)^2$ where $w = 1/\sigma_I^2$. After several cycles of block-diagonal refinement on positional and isotropic thermal parameters, two cycles of full-matrix refinement were undertaken on positional and anisotropic thermal parameters of the platinum, sulfur, and iodine atoms and on the positional and isotropic thermal parameters for the remaining atoms.

At this stage of refinement, it was evident that disorder was present in one of the thiophene rings which was found in the two coplanar orientations shown in Figure 1. Similar disorder is also apparent in the structures of dithienyls.[17] In order to refine this disordered ring satisfactorily, population parameters were chosen for C(16) and S(2) which reflected changes in electron density produced by 25% disorder.

Refinement of positional and isotropic thermal parameters for these atoms resulted in a change of the thermal parameters to values in accord with those of the other carbon and sulfur atoms. Thus sites C(16) and S(2) were simply refined with population parameters 1.414 and 0.845, respectively.

The final positional and thermal parameters and the standard deviations are listed in Tables I and II. A listing of the final observed and calculated structure factors is available.[18]

After the disordered ring was refined on positional and isotropic thermal parameters, the refinement was completed by three cycles of full-matrix least-squares refinement on positional and thermal parameters (anisotropic thermal parameters of the heavier atoms and isotropic thermal parameters of the carbons and nitrogens). The Cruickshank[19] weighting method, $w = 1/(2F_{\min} + F_o + 0.01F_o^2)$, where $2F_{\min} = 54.2$, was introduced and refinement continued to convergence. The residuals at this point R and R_w were 4.6 and 6.1, respectively. A final difference Fourier map contained regions of electron density of 0.8–1.5 e/Å^3 near the platinum site which were attributed to series termination effects. No peaks greater than 0.7 e/Å^3 appeared anywhere else in the map.

Description of the Structure

The structure consists of monomeric units of Pt(TP)(TP-H)I. The closest Pt–Pt distance is 7.48 (1) Å. The bond lengths, angles, and selected intramolecular distances are listed in Tables III–V, respectively. A drawing of the structure is found in Figure 2 and a drawing of the unit cell in Figure 3.

The platinum atom is surrounded by four atoms which approximate a plane. One of the TP groups is coordinated to the platinum through the pyridyl nitrogen and the carbon in the thiophene ring ortho to the bond between the rings. The thiophene ring of the other TP is in an axial position. It is this thiophene ring which is disordered.

The Pt–C(7), Pt–N(1), and Pt–N(2) bond lengths are in accord with values reported for platinum–carbon[20,21] and platinum–nitrogen[21–23] bond lengths in other complexes. The N(1)–Pt–C(7) bond angle of 80.4 (5)° is reasonable based on bond angles which have been reported to vary from 72 to 80° in bipyridyl complexes.[24] The nitrogen atoms lie trans to one another. The Pt–I bond length of 2.68 (1) Å is longer than the Pt–I bond lengths of 2.614 (4) and 2.615 (4) Å reported for Pt(EDM)I_2.[25] In Pt$(TP)_2$I the iodine lies trans to a carbon; in Pt(EDM)I_2 the iodines lie trans to nitrogens. By analogy with phenyl and methyl carbons, thienyl carbons are expected

Table II. Final Thermal Parameters for Pt(TP)(TP-H)I[a,b]

Atom	U_{11}	U_{22}	U_{33}	U_{12}	U_{13}	U_{23}
Pt	328 (3)	357 (3)	388 (3)	14 (3)	65 (2)	20 (3)
I	648 (8)	534 (7)	529 (7)	74 (6)	243 (6)	79 (6)
S(1)	768 (35)	824 (4)	701 (34)	−28 (32)	424 (29)	86 (32)
S(2)/C(16′)	735 (43)	653 (44)	674 (42)	−17 (36)	101 (34)	−119 (35)

Atom	*B*, Å^2	Atom	*B*, Å^2	Atom	*B*, Å^2
N(1)	3.22 (25)	C(7)	3.90 (31)	C(13)	4.79 (40)
C(1)	4.44 (37)	C(8)	4.30 (36)	C(14)	3.02 (27)
C(2)	5.97 (49)	C(9)	5.50 (46)	C(15)	3.10 (29)
C(3)	4.70 (37)	N(2)	3.22 (24)	C(16)/S(2′)	4.75 (28)
C(4)	4.75 (40)	C(10)	4.40 (37)	C(17)/C(18′)	6.57 (53)
C(5)	4.16 (35)	C(11)	4.85 (41)	C(18)/C(17′)	5.57 (47)
C(6)	3.85 (32)	C(12)	5.01 (40)		

[a] Anisotropic values are $\times 10^4$. [b] The form of the anisotropic thermal ellipsoid is $\exp[-2\pi^2(U_{11}h^2a^{*2} + U_{22}k^2b^{*2} + U_{33}l^2c^{*2} + 2U_{12}hka^*b^*\cos\gamma^* + 2U_{13}hla^*c^*\cos\beta^* + 2U_{23}klb^*c^*\cos\alpha^*)]$.

Table III. Intramolecular Bond Lengths for Pt(TP)(TP-H)I

Bond	Length, Å	Bond	Length, Å
Pt-I	2.68 (1)	C(9)-S(1)	1.78 (2)
Pt-N(1)	2.04 (1)	C(6)-S(1)	1.72 (2)
Pt-N(2)	2.02 (1)	N(2)-C(10)	1.38 (2)
Pt-C(7)	1.97 (2)	N(2)-C(14)	1.36 (2)
N(1)-C(1)	1.34 (2)	C(10)-C(11)	1.42 (3)
N(1)-C(5)	1.39 (3)	C(11)-C(12)	1.40 (3)
C(1)-C(2)	1.37 (3)	C(12)-C(13)	1.36 (3)
C(2)-C(3)	1.42 (4)	C(13)-C(14)	1.40 (3)
C(3)-C(4)	1.27 (4)	C(14)-C(15)	1.46 (2)
C(4)-C(5)	1.40 (3)	C(15)-C(16)[a]	1.57 (2)
C(5)-C(6)	1.47 (3)	C(16)-C(17)[a]	1.57 (3)
C(6)-C(7)	1.37 (3)	C(17)-C(18)[a]	1.35 (3)
C(7)-C(8)	1.42 (3)	C(18)-S(2)[a]	1.69 (3)
C(8)-C(9)	1.35 (4)	C(15)-S(2)[a]	1.72 (2)

[a] Averaged value.

Table IV. Intramolecular Angles in Pt(TP)(TP-H)I

Angle	Value, deg	Angle	Value, deg
I-Pt-N(1)	97.9 (4)	N(1)-C(5)-C(6)	111 (2)
I-Pt-N(2)	87.9 (4)	C(5)-C(6)-C(7)	117 (2)
I-Pt-C(7)	176.0 (4)	C(5)-C(6)-S(1)	128 (2)
N(1)-Pt-C(7)	80.6 (7)	S(1)-C(6)-C(7)	114 (1)
N(1)-Pt-N(2)	174.1 (7)	C(6)-C(7)-C(8)	110 (2)
N(2)-Pt-C(7)	93.6 (7)	C(7)-C(8)-C(9)	115 (2)
C(7)-Pt-S(2)	94.8 (5)	C(8)-C(9)-S(1)	110 (2)
N(1)-Pt-S(2)	105.2 (4)	C(9)-S(1)-C(6)	90 (1)
N(2)-Pt-S(2)	74.4 (4)	C(10)-N(2)-C(14)	119 (1)
Pt-N(1)-C(1)	128 (1)	C(11)-C(12)-C(13)	122 (2)
Pt-N(1)-C(5)	115 (1)	C(12)-C(13)-C(14)	119 (2)
Pt-N(2)-C(10)	112 (1)	C(13)-C(14)-N(2)	122 (1)
Pt-N(2)-C(14)	128 (1)	C(14)-C(15)-C(16)	122 (1)
C(1)-N(1)-C(5)	117 (2)	C(14)-C(15)-S(2)	124 (1)
N(1)-C(1)-C(2)	124 (2)	S(2)-C(15)-C(16)	113 (1)
C(1)-C(2)-C(3)	116 (2)	C(15)-C(16)-C(17)	100 (1)
C(2)-C(3)-C(4)	124 (2)	C(16)-C(17)-C(18)	119 (2)
C(3)-C(4)-C(5)	118 (2)	C(17)-C(18)-S(2)	113 (2)
C(4)-C(5)-N(1)	121 (2)	C(18)-S(2)-C(15)	94 (1)
C(4)-C(5)-C(6)	127 (2)		

Table V. Important Nonbonded Intramolecular Distances in Pt(TP)(TP-H)I

Atoms	Distance, Å	Atoms	Distance, Å
Pt-S(2)	2.99 (3)	N(1)-S(2)	4.04 (4)
N(1)-C(7)	2.59 (2)	N(2)-S(2)	3.12 (2)
N(2)-C(7)	2.91 (3)	C(7)-S(2)	3.71 (2)
N(1)-I	3.58 (2)	I-S(2)	3.98 (3)
N(2)-I	3.30 (1)	Pt-C(10)	2.86 (2)
N(1)-N(2)	4.06 (2)	Pt-C(14)	3.06 (2)
Pt-C(16)	2.84 (3)	Pt-S(1)	4.44 (3)
		Pt-C(8)	3.12 (2)

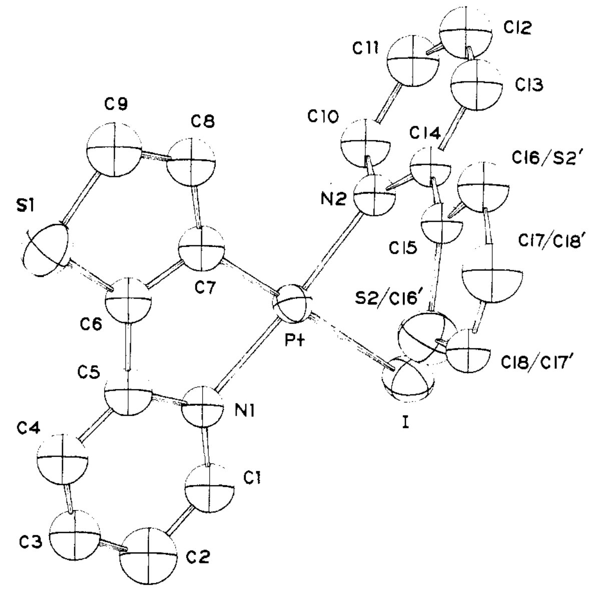

Figure 2. Molecular geometry of Pt(TP)(TP-H)I.

Table VI. Least-Squares Planes and Deviations from the Planes[a]

Plane	Atom	Dev, Å	Plane	Atom	Dev, Å
1	Pt	0.009	2	Pt	−0.025
	N(1)	−0.005		N(1)	−0.035
	N(2)	−0.005		N(2)	−0.034
	C(7)	0.000		C(7)	0.056
3	C(6)	−0.004		I	0.038
	C(7)	−0.001	4	C(15)	0.006
	C(8)	0.007		C(16)/S(2′)	−0.009
	C(9)	−0.008		C(17)/C(18′)	0.009
	S(1)	0.006		C(18)/C(17′)	−0.005
				S(2)/C(16′)	−0.001

[a] Equations defining planes in direct space: (1) $8.40X + 3.76Y + 7.24Z = 2.68$; (2) $8.88X + 3.93Y + 6.72Z = 2.85$; (3) $8.10X + 3.44Y + 7.73Z = 2.47$; (4) $16.09X + 0.48Y - 9.12Z = 2.38$.

to be stronger trans directors than amino nitrogens. Pt–Cl and Pt–Br bond lengths have been found to be longer when the halogen lies trans to a strong trans-directing ligand.[26] It is reasonable to expect similar results for Pt–I bonds.

The iodine position is 0.19 Å below the plane formed by the platinum and the three light coordinating atoms. The deviations of the platinum and all four coordinating atoms from calculated least-squares planes and the deviations of the atoms forming the planes are listed in Table VI. The deviation of the iodine from the least-squares plane appears to be the result of steric effects. The sum of the ionic radius of iodide ion and the van der Waals radius of nitrogen is 3.65 Å.[28] The distance from either nitrogen to the iodine is less than this value. The distance between the iodine and the nitrogens would be even less if these atoms were coplanar.

During the early stages of refinement, it was noted that the isotropic temperature factor of C(16) was lower than the temperature factors of any other carbon and the isotropic temperature factor of S(2) was somewhat higher than the temperature factor of S(1). After completion of the full-matrix cycles, the temperature factor for C(16) was 2.6 Å^2. Temperature factors of other carbons were in the approximate range 4–7 Å^2. In addition, the bond lengths and angles for this ring were found to be significantly different from the bond lengths and angles reported for thiophene[17] or for the chelated thiophene ring in this complex. The difference Fourier calculated at this stage of refinement showed regions of electron density of 1.2–1.5 e/Å^3 surrounding the C(16) site indicating that there was more electron density at this site than was predicted by the model.

These same abnormalities were reported in the structure of 3,3′-dithienyl by Visser et al.[17] and cited as evidence for disorder in the thiophene rings (Figure 4a).

Refinement of our structure as described above improved the temperature factors of these atoms although the bond lengths and angles of the atoms in the disordered ring remained essentially unchanged. The values reported for bond lengths and angles represent averages between the actual values of the atoms at a given site in each orientation (Figure 4c). By analogy with the compounds described by Visser, in which rings in both orientations lie on the same plane, the orientations of the disordered ring in Pt(TP)(TP-H)I are also taken to be coplanar. This is supported by the fact that the atom positions in the ring, which represent averages, show no significant deviations from planarity (Table VI).

The reported Pt–S(2) distance of 2.99 (3) Å is, of course, an average of actual Pt–S(2) and Pt–C(16′) distances. Inspection of Figure 4 reveals that the bond lengths and angle at the position S(2)/C(16′) have values which are much closer to C–S bond lengths and C–S–C bond angles than C–C and

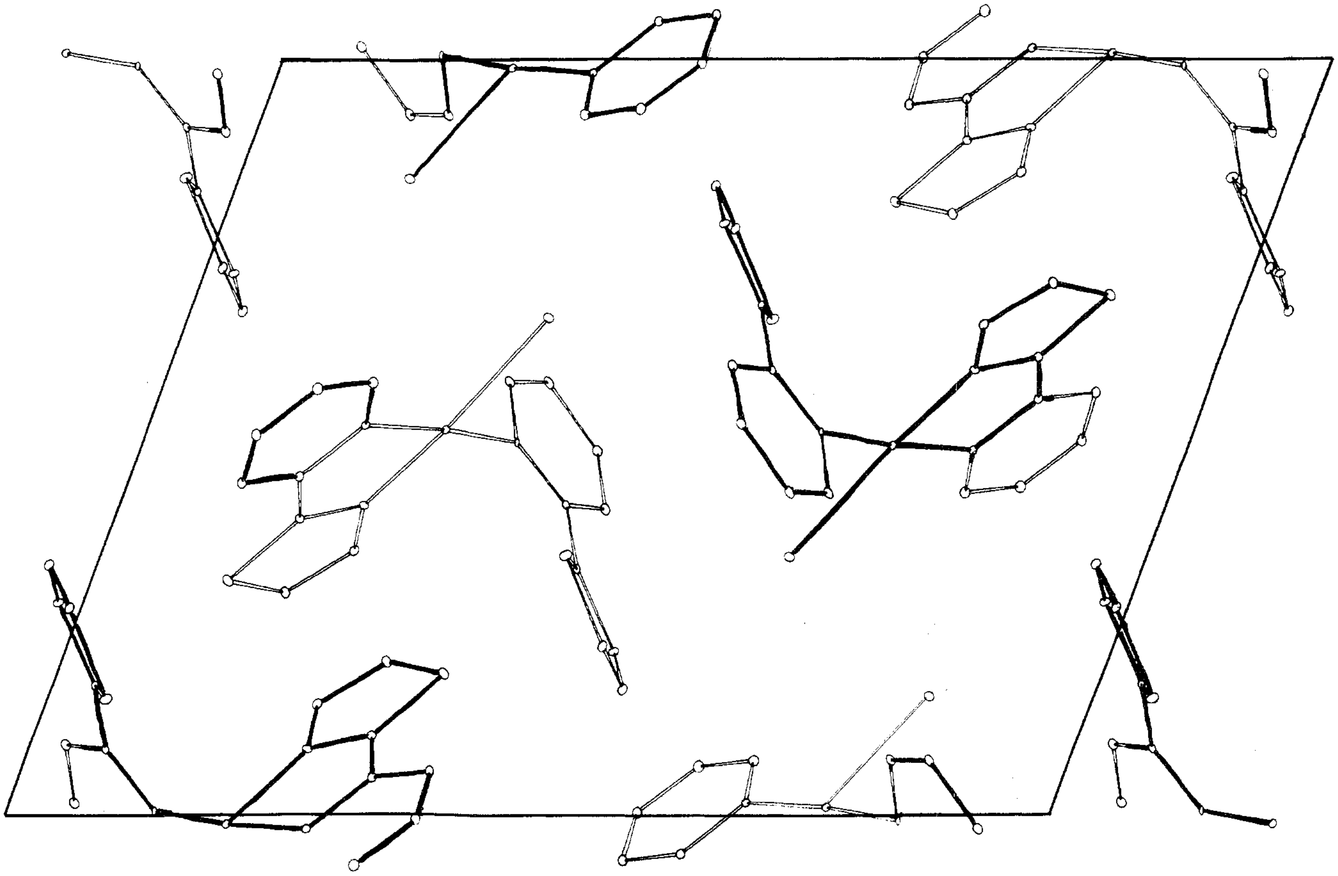

Figure 3. Packing of Pt(TP)(TP-H)I projected on the 010 plane.

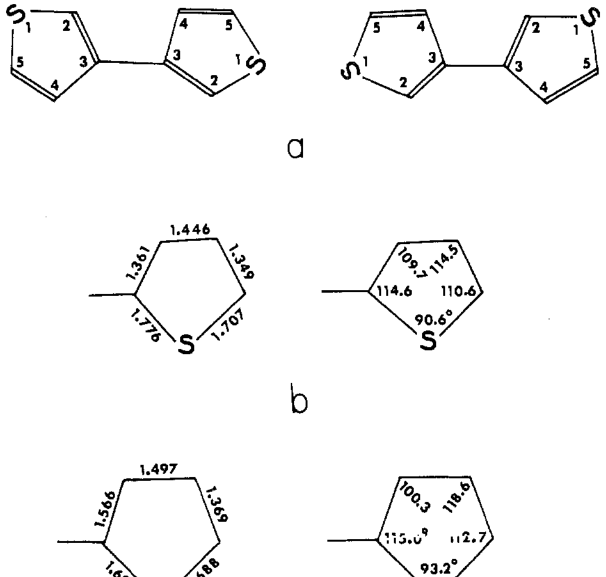

Figure 4. (a) Disorder in 3,3′-dithienyl; (b) bond lengths and angles proposed for the disordered ring; (c) bond lengths and angles found based on average orientation.

C–C–C bond lengths and angles, respectively. Therefore, it is reasonable to assume that the value reported for the Pt–S(2) distance is close to the true value. This distance is less than the sum of the van der Waals radii of sulfur[28] and platinum atoms[29] (3.92 Å) implying interaction between the sulfur and platinum atoms. It is debatable whether this interaction is attractive or repulsive. This distance is much longer than a reported Pt–S bond length of 2.31 Å.[30] Moreover, it might be expected, if there were a Pt–S bond, that all of the sulfurs would point toward the platinum. The N(2)–Pt–S(2) and the C(7)–Pt–S(2) angles of 74.4 (4) and 94.8 (5)°, respectively, indicate that the sulfur does not lie directly above the platinum. The line between the platinum and the sulfur atoms makes an angle of ca. 15° with a line perpendicular to the equatorial plane at the platinum position.

The orientations of the two rings in the unchelated TP are of interest because the thiophene ring is held away from the platinum. The pyridine ring is tilted 12° from being perpendicular to the platinum plane. In addition, there is a difference of 16° between the Pt–N(2)–C(10) and the Pt–N(2)–C(14) bond angles indicating that C(14) is further from the platinum than C(10).

The C–C bonds and the C–S bonds in the chelated thiophene ring are normal.[17] The average C–C and C–N bond lengths in the pyridine rings, 1.36 (2) and 1.38 (3) Å, are also reasonable.[29]

The bond distances between the thiophene and pyridine rings are shorter than the C–C single-bond length of 1.54 Å. This implies a partial double bond between the rings indicating π bonding between them. The rings are not coplanar in either TP group. In the chelated group, the angle between the rings is ca. 5°; in the unchelated TP the corresponding angle is ca. 22°. Similar deviations from coplanarity have been found between pyridine rings in bipyridyl complexes.[24]

The iodine atom lies nearly 0.3 Å closer to N_2 than to N_1. In this latter case a cis interaction with the C_1 hydrogen is evident.

Discussion

On the basis of X-ray powder patterns, as well as similar spectra and properties, Pt(TP)(TP-H)Br is assumed to have the same structure as Pt(TP)(TP-H)I. It is more difficult to draw conclusions concerning the structure of Pd(TP)(TP-H)NO_3 because it is not isomorphous with the platinum

Table VII. Visible–Ultraviolet Absorption Spectra^a

TP	33.3 (140), 37.8 (80.0) sh, >41.7 (>200)
Pt(TP)(TP-H)I	18.5 (0.15), 20.0 (0.28) sh, 24.4 (34.0), 35.4 (200), 37.8 (210), >41.7 (>240)
Pt(TP)(TP-H)Br	18.5 (0.10), 20.0 (0.21) sh, 24.4 (34.0), 33.2 (190), 37.8 (190)
$Pd(TP)(TP-H)NO_3$	27.8 (55.0) sh, 34.0 (180), 38.5 (180), >41.7 (>220)

^{a} All values are in kilokaisers. The values in parentheses are molar extinction coefficients × 10^{-2}. sh = shoulder.

complexes. The elemental analyses, molecular weight, and conductivity measurement are strong evidence that the metal ion is coordinated by chelated and unchelated TP groups and a monodentate nitrate.

Substitution of a phenyl ring by platinum in the complexes containing substituted phosphines is dependent upon the bulk of the phosphine substituents.[5] For example, substitution occurs after 50 hr of heating of *trans*-$Pt(PPh_2t\text{-}Bu)_2Cl_2$ in dimethoxyethanol; *trans*-$Pt(PPh\text{-}t\text{-}Bu_2)_2Cl_2$ requires 10 hr of heating; *trans*-$Pt(PPh_2Me)_2Cl_2$ and $Pt(PPhMe_2)_2Cl_2$ do not undergo substitution.

In the coordination plane of Pt(TP)(TP-H)I crowding is sufficient to force the iodine slightly from the plane. It is reasonable to assume that steric interactions would be greater in a complex of formula $Pt(TP)_2I_2$. Formation of the metal–carbon bond allows release of one halogen and relief of some of the steric repulsions in Pt(TP)(TP-H)I and its bromo isomorph.

It is more difficult to draw any conclusions concerning the formation of $Pd(TP)(TP-H)NO_3$ because its structure is uncertain. It is expected that steric interactions would be less than in the platinum complex because most of the monodentate nitrate is held away from the metal. A possible factor in the formation of the palladium complex is the lability of nitrate ion which could make it susceptible to substitution by a thienyl carbon.

The location of the unchelated thiophene ring near an axial coordination site in Pt(TP)(TP-H)I is consistent with the electronic spectrum of this complex which resembles the spectra of five-coordinate square-pyramidal rather than four-coordinate square-planar d^8 complexes.

The spectrum of Pt(TP)(TP-H)I contains an intense asymmetric band at 24.4 kK. Square-planar platinum(II) complexes such as $PtCl_4^{2-}$,[34] $PtBr_4^{2-}$,[32] and the complexes of the series $Pt(NH_3)_xCl_{4-x}^{(2-x)-}$ [35] have only weak bands in this region ($\epsilon < 100$) which have been assigned to d–d transitions. The energies of these bands are strongly dependent on the positions of the ligands in the spectrochemical series. The spectra of the five-coordinate square-pyramidal complexes of *o*-phenylenebis(dimethylarsine) contain intense bands at relatively low energies. For example, the lowest energy band in square-planar $Ni(diars)_2(ClO_4)_2$ is found at 22.6 kK (ϵ 440).[34] The five-coordinate square-pyramidal complexes $(Ni(diars)_2X)X$ (X = Cl, Br, I) yield more intense bands ($\epsilon \sim 1000$) at 21.3, 21.0, and 20.2 kK, respectively. Gray[32] has postulated that the order of d-orbital energies in these complexes is $xy < xz, yz < z^2 < x^2 - y^2$ and assigned these bands to the transition ${}^1A_1 \rightarrow {}^1E_1$ $(xz, yz \rightarrow x^2 - y^2)$ because it is orbitally allowed in C_{4v} symmetry. Similarly, the five-coordinate complexes $(Pt(diars)_2X)X$ (X = Cl, Br, I) contain bands which are more intense and appear at lower energy than are found in $Pt(diars)_2(ClO_4)_2$.[35]

The Pt–S(2) distance is less than the sum of their van der Waals radii, which is direct evidence of axial interaction in Pt(TP)(TP-H)I. Axial interaction would be expected to raise the energy of the d orbitals which have components in the *z* direction relative to those which do not. This could explain why the ligand field bands are found at relatively low energy.

The presence of a similar band in the spectrum of the isomorphous Pt(TP)(TP-H)Br at 24 kK is evidence that the axial interactions are comparable. On the basis of the foregoing spectral and structural evidence these bands are assigned to d–d transitions whose energy has been lowered and intensity increased by the axial interaction of a thiophene ring with the metal. The analogy to five-coordinate complexes as well as the asymmetry of this band suggests that the transitions are $d_{xz}, d_{yz} \rightarrow d_{x^2-y^2}$. An intense band is found in the spectrum of $Pd(TP)(TP-H)NO_3$ at 27.0 kK, which is also assumed to be a result of axial interaction.

The weak bands found in the spectra of the platinum complexes at 20 kK are tentatively assigned to spin-forbidden d–d transitions on the basis of their intensities. The intense band found near 34 kK in assigned to a ligand-based transition because it is found in the spectrum of the free ligand.

The spectra of the complexes containing a chelated TP contain a band at ca. 38 kK of intensity approximately equal to that of the aforementioned ligand band. Therefore it is assigned to a ligand-based transition of the chelated ligand. Any bands found at higher energies are assigned to charge-transfer and ligand bands.

See Table VII for the ultraviolet–visible absorption spectra of TP, Pt(TP)(TP-H)I, Pt(TP)(TP-H)Br, and $Pd(TP)(TP-H)NO_3$.

The ir spectrum of TP contains a strong band at 850 cm^{-1}. The spectra of thiophene and 2-substituted thiophenes contain one or more strong bands in this region.[36] The spectra of pyridine and 2-substituted pyridines are empty in this region.[37] Therefore, the band at 850 cm^{-1} is assigned to a thiophene vibration. This band is shifted to 875 cm^{-1} in the complexes described here.

We prefer to describe these complexes as four-coordinate with axial interactions rather than five-coordinate with metal–sulfur or metal–thiophene axial bonds. The high reactivity of the thiophene ring and the possibility of chelation leads to formation of a metal–carbon bond under unusually mild conditions and in the presence of air and water.

Registry No. TP, 3319-99-1; Pt(TP)(TP-H)I, 54751-63-2; Pt(TP)(TP-H)Br, 54751-64-3; $Pd(TP)(TP-H)NO_3$, 54751-65-4.

Supplementary Material Available. A listing of structure factor amplitudes (Table VIII) will appear following these pages in the microfilm edition of this volume of the journal. Photocopies of the supplementary material from this paper only or microfiche (105 × 148 mm, 24× reduction, negatives) containing all of the supplementary material for the papers in this issue may be obtained from the Journals Department, American Chemical Society, 1155 16th St., N.W., Washington, D.C. 20036. Remit check or money order for $4.50 for photocopy or $2.50 for microfiche, referring to code number AIC40725Q.

References and Notes

(1) G. Parshall, *Acc. Chem. Res.*, **3**, 139 (1970), and references contained therein.
(2) A. C. Cope and R. W. Siekman, *J. Am. Chem. Soc.*, **87**, 3272 (1965).
(3) A. Kasahara, *Bull. Chem. Soc. Jpn.*, **41**, 1272 (1968).
(4) A. C. Cope and E. C. Friederich, *J. Am. Chem. Soc.*, **90**, 909 (1968).
(5) A. J. Cheney, B. E. Mann, B. C. Shaw, and R. M. Slade, *J. Chem. Soc. A*, 3833 (1971).
(6) T. J. Giordano, Ph.D. Thesis, University of Michigan, 1974.
(7) E. D. Olsen, R. S. Martin, and S. E. Ahnell, *J. Chem. Educ.*, **47**, 542 (1970).
(8) H. J. Garrett and R. E. Brocklehurst, "Tables of Interplanar Spacings", ASTIA Document Service, Dayton, Ohio, 1958.
(9) T. Kauffmann, E. Wienhofer, and A. Woltermann, *Angew. Chem., Int. Ed. Engl.*, **10**, 741 (1971).
(10) "International Tables for X-Ray Crystallography", Vol. II, Kynoch Press, Birmingham, England, p 302.
(11) J. M. Stewart, F. A. Kundell, and J. C. Baldwin, "The X-ray System of Crystallography Programs", University of Maryland, 1972.
(12) J. W. Schilling, "Fortran IV Crystallographic Least Squares Program", University of Michigan, Dec 1965.
(13) C. K. Johnson, "ORTEP: a Fortran Thermal Ellipsoid Program for Crystal Structure Illustrations", Oak Ridge National Laboratory, Oak Ridge, Tenn., 1965.

(14) D. T. Cromer and J. T. Waber, *Acta Crystallogr.*, **18**, 104 (1965).
(15) R. F. Stewart, J. T. Davidson, and W. T. Simpson, *J. Chem. Phys.*, **42**, 3175 (1965).
(16) "International Tables for X-Ray Crystallography", Vol. II, Kynoch Press, Birmingham, England, p 202.
(17) G. J. Visser, G. J. Heeres, J. Walters, and A. Vos, *Acta Crystallogr., Sect. B*, **24**, 467 (1968).
(18) Supplementary material.
(19) D. W. J. Cruickshank et al., "Computing Methods and the Phase Problem in X-Ray Crystal Analysis", R. Pepinsky et al., Ed., Pergamon Press, Oxford, 1961.
(20) E. M. Bradley, J. Chatt, R. L. Richards, and G. A. Sim, *J. Chem. Soc. D*, 1322 (1969).
(21) C. Panattoni, R. Bombiere, E. Forsellini, B. Crocioni, and V. Belluco, *J. Chem. Soc. D*, 187 (1969).
(22) B. M. Craver, and D. Hall, *Acta Crystallogr.*, **21**, 177 (1966).
(23) D. Moros, J. Dehand, and R. Weiss, *C. R. Hebd. Seances Acad. Sci., Ser. C*, **276**, 1471 (1968).
(24) V. G. Albano, P. L. Bellon, and M. Sansori, *Inorg. Chem.*, **8**, 298 (1969), and references contained therein.
(25) W. Eventoff, Ph.D. Thesis, University of Michigan, 1972.
(26) F. Basolo and R. G. Pearson, "Mechanisms of Inorganic Substitution", Wiley, New York, N.Y., 1967, pp 351–375.
(27) G. H. Stout and L. H. Jensen, "X-Ray Structure Determination", Macmillan, New York, N.Y., 1968, pp 421–425.
(28) F. A. Cotton and G. Wilkinson, "Advanced Inorganic Chemistry", 2nd ed, Interscience, New York, N.Y., 1967, pp 45, 115.
(29) N. C. Stephenson, *J. Inorg. Nucl. Chem.*, **24**, 791 (1962).
(30) J. P. Beale and N. C. Stephenson, *Acta Crystallogr., Sect. B*, **27**, 73 (1971).
(31) "International Tables for X-Ray Crystallography", Vol. II, Kynoch Press, Birmingham, England, 1962, p 276.
(32) W. R. Mason, III, and H. B. Gray, *J. Am. Chem. Soc.*, **90**, 5721 (1968).
(33) J. Chatt, G. A. Gamelin, and L. E. Orgel, *J. Chem. Soc.*, 486 (1958).
(34) J. R. Preer and H. B. Gray, *J. Am. Chem. Soc.*, **92**, 7306 (1970).
(35) G. Dolcetti, A. Peloso, and L. Sindarelli, *Gazz. Chim. Ital.*, **96**, 1948 (1966).
(36) A. R. Katritzky and A. P. Ambler, "Physical Methods in Heterocyclic Chemistry", Vol. 2, A. R. Katritzky, Ed., Academic Press, New York, N.Y., 1963, pp 205–208.
(37) O. H. S. Greer, W. Kynaston, and H. M. Paisley, *Spectrochim. Acta*, **19**, 549 (1963).

Contribution from the Department of Chemistry,
Polytechnic Institute of New York, Brooklyn, New York 11201

Crystal Chemistry of Struvite Analogs of the Type $MgMPO_4 \cdot 6H_2O$ ($M^+ = K^+, Rb^+, Cs^+, Tl^+, NH_4^+$)[1]

E. BANKS,* R. CHIANELLI,[2a] and R. KORENSTEIN[2b]

Received September 4, 1974 AIC40631G

The crystallographic properties and the infrared absorption spectra of the struvite analogs of the type $MgMPO_4 \cdot 6H_2O$ where $M^+ = K^+$, Rb^+, Cs^+, Tl^+, or NH_4^+ are reported. The relative stabilities of the struvite analogs are discussed in terms of the radii of the univalent ions.

I. Introduction

The mineral struvite ($MgNH_4PO_4 \cdot 6H_2O$) is often found associated with living or decomposing organisms. It has been described in ref 3 as being found in dung, putrescent matter, canned foods, and bladder or kidney concretions. The crystal structure was solved with a crystal obtained from a tin of salmon. This structure was based on the earlier work of Bland and Basinski[4] and Whitaker and Jeffery.[5,6] The analogous compound $MgKPO_4 \cdot 6H_2O$ was reported as forming an isomorphous series with struvite by Lehr et al.[7] The infrared spectra, X-ray diffraction patterns, and optical and crystallographic properties of struvite and the potassium analog were also reported. Struvite has been compared to the related compound $CaKAsO_4 \cdot 8H_2O$,[8] and their biological importance as possible precursors of nuclei of crystallization has been noted. The apparently related materials $MgCsPO_4 \cdot 6H_2O$ and $MgCsAsO_4 \cdot 6H_2O$ have also been reported by Ferrari et al.[9,10] It is the purpose of this report to study the substitution of alkali metals and "pseudoalkali" cations in the struvite crystal structure.

II. Experimental Section

All crystals were grown by means of the gel diffusion technique. The growth of struvite by the gel diffusion method has been reported by Banks et al.[11,12] An aqueous solution of 0.05 *M* $MgSO_4$ and 0.04–0.02 *M* M_2EDTA (EDTA = ethylenediaminetetraacetate) was adjusted to pH 10 with MOH. Eastman Kodak "ultrapure" calfskin gelatin was dissolved in the resulting solution (55 g/l.) and allowed to set. Before setting, several drops of formaldehyde were added to strengthen the gel and to prevent growth of molds. Generally 100 ml of gel was set in a 250-ml electrolytic beaker. When the gel had set an equivalent amount of a solution of 0.05 *M* $M_2HPO_4 \cdot xH_2O$ which had been adjusted to pH 10.0 with MOH was carefully poured over the gel. The beaker was covered and the crystal growth proceeded at the gel–liquid interface and into the gel. Experiments were complete within several weeks and the crystals were harvested. Photographs of the resulting crystals may be seen in Figure 1.

All reagents used were Baker Analyzed reagents except the Eastman Kodak calfskin gelatin. Rubidium and cesium phosphates were prepared by neutralizing H_3PO_4 with an equivalent amount of RbOH or CsOH in situ. Rubidium, ammonium, potassium, and cesium salts of EDTA were prepared by neutralizing H_2EDTA with an equivalent amount of RbOH or CsOH also in situ. In the case of the thallium salt $TlNO_3$ was used as a source of thallium and Na_2EDTA and NaOH were used. The presence of sodium did not interfere with the growth of $MgTlPO_4 \cdot 6H_2O$ or any of the other struvite analogs and Na_2EDTA can replace the M_2EDTA.

X-Ray powder patterns were taken on a Norelco powder diffractometer with monochromated Cu Kα radiation with KCl as an internal standard.

Infrared spectra were taken on a Perkin-Elmer Model 521 spectrometer with the sample in a KBr disk.

Crystal densities were measured either by pycnometric means or by the sink–float method.[13]

Chemical analyses were performed by Galbraith Laboratories Inc., Knoxville, Tenn.

Crystal size and perfection can be optimized by varying the conditions described above. Table I shows the best conditions tried for each material and the results obtained.

III. Crystallographic Properties

Crystals of struvite occurred in both wedge-shaped prisms and needles. Twins on (001) such as described by Palache et al.[3] are frequently seen. Both $MgKPO_4 \cdot 6H_2O$ and $MgRbPO_4 \cdot 6H_2O$ were seen only in needle form. $MgTlPO_4 \cdot 6H_2O$ grew in wedge-shaped, distinctly struvite-like crystals and in other shapes. Crystals of $MgCsPO_4 \cdot 6H_2O$ were capped hexagonal prisms or trigonal pyramids as described by Ferrari et al.[9,10] All crystals were stable for short periods when taken from their mother liquor except $MgRbPO_4 \cdot 6H_2O$ which clouded easily. Struvite crystals may be stored in a capped bottle indefinitely but all other crystals showed a tendency to hydrolyze to a greater or lesser extent over long periods of time. However, the NH_4^+, Tl^+, and Cs^+ crystals showed a greater degree of stability than the K^+ or Rb^+ crystals. Table II